Neurobiology of Aging 76 (2019) 62–70

Contents lists available at ScienceDirect

Neurobiology of Aging

journal homepage: www.elsevier.com/locate/neuaging

# The longitudinal decline of white matter microstructural integrity in behavioral variant frontotemporal dementia and its association with executive function

Junhong Yu [a,b], Tatia M.C. Lee [a,b,c,*], for the Frontotemporal Lobar Degeneration Neuroimaging Initiative[1]

[a] The State Key Laboratory of Brain and Cognitive Sciences, Department of Psychology, The University of Hong Kong, Hong Kong
[b] Laboratory of Neuropsychology, Department of Psychology, The University of Hong Kong, Hong Kong
[c] Institute of Clinical Neuropsychology, Department of Psychology, The University of Hong Kong, Hong Kong

ARTICLE INFO

*Article history:*
Received 31 July 2018
Received in revised form 23 November 2018
Accepted 15 December 2018
Available online 25 December 2018

*Keywords:*
Frontotemporal dementia
Executive function
DTI
White matter
Corpus callosum

ABSTRACT

The longitudinal decline in the integrity of several white matter (WM) tracts in behavioral variant frontotemporal dementia (bvFTD) has been documented. However, there is yet a clear relationship between this decline and that of executive function (EF), for the WM changes to meaningfully track progression in bvFTD. We sought to validate the use of diffusion tensor imaging (DTI) in tracking the progression of bvFTD with its associated decline in EF. Baseline and 1-year follow-up DTI scans were acquired from 23 patients with bvFTD and 26 healthy controls. EF composite score was derived via multiple tests. The longitudinal changes in DTI metrics were examined in both groups. Then, among patients (N = 18), we examined the associations between these changes and that of EF. Widespread WM alterations and decline in EF were observed only in patients. This EF decline was mostly associated with the disrupted integrity of the corpus callosum and anterior corona radiata. These longitudinal findings support the use of DTI in tracking the progression of bvFTD and its associated EF decline.



## 1. Introduction

Behavioral variant frontotemporal dementia (bvFTD)—the most common type of frontotemporal dementia (FTD; Bang et al., 2015)—is characterized by the progressive deterioration of personality and social behaviors. Neuropsychologically, patients with bvFTD present with deficits in executive function (EF), whereas memory and visuospatial functions may be relatively spared. Progression in bvFTD varies across patients. Some patients, typically referred to as "phenocopy" cases experience little to no progression across time in terms of cognitive abilities and functional status (Devenney et al., 2015). On the other hand, patients found to possess the hexanucleotide expansion in the C9orf72 gene experience a relatively rapid frontal lobe degeneration and decline in cognitive abilities (Irwin et al., 2012). Given the variability of progression in bvFTD, the importance of tracking its progression for timely intervention and prediction of prognosis cannot be understated.

Relatedly, there has been some recent research involving the use of diffusion tensor imaging (DTI) to track the progression of bvFTD. The use of DTI to study bvFTD is justified by the fact that it measures the microstructural integrity of white matter (WM) tracts; neurobiological processes in the 3 different types of pathologies commonly associated with bvFTD—tau, TAR DNA-binding protein 43, and fused in sarcoma—can adversely affect this microstructural integrity. In the first type, tau deposits into neurons and glia to form neurofibrillary tangles that affects not only gray matter (GM) but WM as well (Ghetti et al., 2015); these tangles have been prominently observed in glia cells of the deep WM tracts and internal capsule (Mann and Snowden, 2017), suggesting the presence of axonal degeneration (Leyns and Holtzman, 2017). In the TAR DNA-binding protein 43 and fused in sarcoma pathologies, glial cytoplasmic inclusions are present in the WM (Mackenzie and Neumann, 2016), whose presence was correlated with WM damage, specifically in the myelination of WM (Powers et al., 2003). Furthermore, DTI metrics could potentially be more helpful than GM variables (e.g., frontal lobe atrophy) in

* Corresponding author at: Laboratory of Neuropsychology, Department of Psychology, The University of Hong Kong, Rm 656, Jockey Club Tower, Pokfulam Road, Hong Kong. Tel: +852-39178394; fax: +852-28583518.
*E-mail address:* tmclee@hku.hk (T.M.C. Lee).

[1] Data used in preparation of this article were obtained from the Frontotemporal Lobar Degeneration Neuroimaging Initiative (FTLDNI) database (http://4rtni-ftldni.ini.usc.edu/). The investigators at NIFD/FTLDNI contributed to the design and implementation of FTLDNI and/or provided data but did not participate in analysis or writing of this report (unless otherwise listed).


https://doi.org/10.1016/j.neurobiolaging.2018.12.005

aiding diagnostic decisions, as one study has shown that DTI metrics were significantly more accurate than GM atrophy in classifying FTD subtypes (Zhang et al., 2013).

The limited longitudinal research on bvFTD has generally observed the significant decline in the integrity of several WM tracts. Two studies, analyzing whole-brain tract-based spatial statistics, reported significant deterioration of WM microstructural integrity, in terms of decrease fractional anisotropy (FA) and increased mean diffusivity (MD), in patients with bvFTD over an approximately 1-year follow-up period. Specifically, these WM changes were observed extensively throughout several WM tracts in one study (Lam et al., 2014) and mostly in the frontal WM in the other (Elahi et al., 2017). A third study, using another whole-brain approach to compare the 1-year longitudinal changes in FA between healthy controls and patients with bvFTD, has observed significant FA decrease in the frontal WM of patients with bvFTD relative to healthy controls (Kassubek et al., 2018). Finally, a fourth study, using an atlas-based regions of interest (ROIs) approach, found significant FA decrease and MD increase in the corpus callosum (CC), cingulum, uncinate fasciculus, and superior cerebellar peduncle among patients with bvFTD over a 1.3-year follow-up period (Mahoney et al., 2015). In general, these studies evidenced a significant longitudinal decline in WM microstructural integrity among patients with bvFTD, although they might differ to a small extent, in the specific WM regions affected.

To improve the utility of DTI metrics in tracking the progression of the disease, it is important to map the observed longitudinal changes to measurable changes in symptoms severity. From a clinical standpoint, this would mean the changes in daily functioning or severity of symptoms such as apathy, disinhibition, or inappropriate social behaviors. However, these variables may not be easily or meaningfully quantified, especially if one intends to relate these variables to DTI metrics. Instead, we chose to look at EF. EF deficits are a central cognitive feature of bvFTD (Piguet et al., 2011), hence can be used to approximate progression in the condition. Furthermore, EF can be objectively measured and easily quantified via various neuropsychological tests. In this regard, there has yet to be longitudinal studies demonstrating an association between decline in EF and the deterioration in WM microstructural integrity, although 2 cross-sectional studies have reported associations between EF tests and FA in the uncinate fasciculus, forceps minor (Hornberger et al., 2011), and anterior cingulum (Tartaglia et al., 2012) among patients with bvFTD. To address this research gap, this study used the publicly available Frontotemporal Lobar Degeneration Neuroimaging Initiative (FTLDNI) data set to examine the longitudinal association between WM microstructural integrity and EF decline. This research goal was achieved via a few steps. First, we showed that there was indeed a longitudinal decline in the WM microstructural integrity in bvFTD not attributable to normal aging. This was exemplified by showing significant decrease in FA and increase in MD across time only in patients with bvFTD but not healthy controls. Second, to measure EF accurately in bvFTD, we created and validated an EF composite score, incorporating test scores from multiple EF tests. Finally, we correlated changes in this EF composite score with WM microstructural changes across time in bvFTD. For the first and final steps, we hypothesized that there were significant clusters of FA decrease and MD increase in the frontal WM regions, and these clusters were significantly correlated with changes in EF composite scores across time.

## 2. Material and methods

Data used in the preparation of this article were obtained from the FTLDNI database. The FTLDNI is funded through the National Institute of Aging, and started in 2010. The primary goals of FTLDNI are to identify neuroimaging modalities and methods of analysis for tracking frontotemporal lobar degeneration and to assess the value of imaging versus other biomarkers in diagnostic roles. The Principal Investigator of FTLDNI is Dr Howard Rosen, MD, at the University of California, San Francisco. The data are the result of collaborative efforts at 3 sites in North America. For up-to-date information on participation and protocol, please visit: http://memory.ucsf.edu/research/studies/nifd.

### 2.1. Participants

For the DTI analyses, we included 26 healthy controls and 23 participants with bvFTD who had valid baseline and follow-up DTI scans approximately 1 year later (±0.25 years). Table 1 presents the characteristics of these 2 groups of participants. Both groups were similar in terms of age, gender ratio, and follow-up duration. As expected, participants with bvFTD had significantly lower Mini-Mental State Examination scores and fewer years of education. The Clinical Dementia Rating scores (language, behavior, total, and box) and Neuropsychiatric Inventory Questionnaire severity scores for each participant with bvFTD are presented in supplementary materials (see Table S1)

To construct the EF composite scores, we included the baseline data of all 326 participants (167 females) in the FTLDNI data set. At baseline, they had a mean age of 63.8 years (SD = 7.2), an average of 16.8 years of education (SD = 2.7) and scored an average of 26.7 on the Mini-Mental State Examination (SD = 4.3). These participants included healthy controls (N = 137) and patients with bvFTD (N = 74) and other FTDs—progressive nonfluent aphasia (N = 38) and semantic-variant FTD (N = 41), as well as 36 patients of other diagnoses. Among them, 170 were assessed approximately 1 year later (±0.25 years; mean follow-up = 1.05 years; SD = 0.1). Their follow-up data were also included for the creation of the EF composite scores.

It should be noted that among the 74 participants with bvFTD included for the derivation of the composite scores, only 26 of them had baseline DTI scans collected within the same period (± 3 days) as their cognitive tests measures. The other 48 participants either did not have any DTI scans or have scans, which were collected too far (>3 months) from the date of cognitive assessments for both types of data to be used meaningfully together. Furthermore, among these 26 participants with time-matched DTI and cognitive test data at baseline, only 23 participants had DTI scans at a 1-year follow-up (as described earlier). Of these, 5 did not have time-matched DTI and cognitive test data at 1-year follow-up period. As a result, we have to exclude these 5 participants for the analyses of the longitudinal associations between WM changes and EF. Finally, among the 137 healthy participants included in the derivation of the EF composite scores, only 26 had valid DTI scans both at baseline and 1-year follow-up (as described earlier).

Participants with FTDs were referred by physicians or self-referred. They underwent comprehensive neurological, neuropsychological, and functional assessments, including informant interview at one of 3 study sites—University of California, San Francisco, Mayo Clinic, Rochester and Massachusetts General Hospital. They were diagnosed using the published consensus criteria

**Table 1**
Characteristics of scanned participants

| Characteristic | Healthy controls | bvFTD |
|---|---|---|
| N | 26 | 23 |
| Mean age (SD) | 62.8 (5.9) | 61.1 (6.5) |
| %Males | 23.1 | 31.8 |
| Mean education in years (SD) | 17.7 (0.9) | 16.1* (3.5) |
| Mean follow-up in years (SD) | 1.1 (0.1) | 1.0 (0.1) |
| Mean MMSE score (SD) | 27.4 (3.3) | 24.1** (4.6) |

Key: bvFTD, behavioral variant frontotemporal dementia; MMSE, mini-mental state examination; SD, standard deviation.
*$p < 0.05$; **$p < 0.01$. Significant $p$ values indicate significant difference from healthy controls using independent samples t-test.

for the various FTDs (Gorno-Tempini et al., 2011; Neary et al., 1998; Rascovsky et al., 2011) at a multidisciplinary consensus conference. Ethics approval for the FTLDNI protocol has been granted by institutional review boards at their respective study sites.

### 2.2. Measures

Participants were assessed on various EF domains. The maximum span scores of the forward and backward digit span tests from the Wechsler Memory Scale III (Wechsler, 1997) were used to measure working memory. Next, participants were assessed on their fluency using the letter fluency (Kramer et al., 2003) and category fluency tests (Lezak, 1995). In these tests, they were given a minute to say aloud, as many as possible words starting with the letter "d" and animals, respectively. The number of correct and unique words was used in this study. Finally, participants were administered the modified trail-making task (Kramer et al., 2003); the completion time was used as a measure of task switching ability. In this modified version, participants alternated between number and day of the week in connecting the circles. Scores for the modified trail-making task have been reversed before entering into the analyses such that higher scores correspond to better EF abilities, as with the other EF tests. These 5 tests were the only EF-related tests included in the FTLDNI data set.

### 2.3. Magnetic resonance imaging acquisition

Participants were scanned using Siemens TrioTim 3T scanners at the study sites. DTI images were acquired with an echo-planar imaging spin echo protocol (Echo time = 82 ms; Repetition time = 9.2s; 896 × 560 matrix, 45 axial slices, in-plane resolution = 2.7 mm; slice thickness = 2.7 mm; 44 diffusion-weighted volumes; b-value = 1000 s/mm$^2$).

### 2.4. Image processing

The raw diffusion images were skull-stripped and corrected for eddy current and subject movement using FMRIB Software Library (FSL 5.0.8). Then, we used an unbiased approach as similarly described in the study by Keihaninejad et al. (2013) for the longitudinal registration. Diffusion tensors were then generated for each participant for the registration of the diffusion tensors. For each subject, a within-subject template was generated by computing the initial average template as a Log-Euclidean mean of the baseline and follow-up diffusion tensors. This template was iteratively refined; the diffusion tensors were registered to the template, and a refined average template was similarly computed from the 2 registered diffusion tensors for the next iteration. The process was repeated until the difference between templates from consecutive iterations became sufficiently small; first with affine and then with nonlinear registrations. Next, a study template was created, separately for healthy controls and participants with bvFTD, from all the final average templates in the within-subject space using the same iterative method. Then, FA and MD maps were generated from each registered tensor image in their respective study template space. These preprocessing steps were carried out using the DTI toolkit. Finally, a mean FA image representing the centers of all tracts common to the group, thresholded at FA > 0.30, was created and each subject's aligned FA and MD images were projected onto this mean FA image to obtain their skeleton images.

### 2.5. Statistical analyses

To study the longitudinal changes in WM microstructural integrity within each group, we performed, separately on healthy controls and participants with bvFTD , single-group paired t-tests on the FA and MD images through a general linear model (GLM). Contrasts for baseline > follow-up and follow-up > baseline were set up for this GLM. Next, to identify WM regions longitudinally associated with EF among the patients (N = 18) with valid DTI and EF data, we computed the differences across time (follow-up−baseline) for FA, MD, and EF scores. Then, a single-group average with additional covariates GLM was set up to examine the associations between the FA/MD difference images and EF difference scores while incorporating age, sex, and education as covariates. For these analyses, GLM contrasts for both positive and negative correlations were set up. The GLM setups were then subjected to 5000 random nonparametric permutations using the 2D parameter settings with threshold-free cluster enhancement to obtain the test statistics (Winkler et al., 2014). These statistical maps were then thresholded using family-wise error corrected $p < 0.05$. Subsequently, they were warped on to the FMRIB58_FA space before extracting labels from the JHU ICBM-DTI-81 atlas. Furthermore, if significant results were obtained for any of the analyses involving MD, these analyses were then repeated with radial diffusivity (RD) and axial diffusivity (AxD) measures to further assess the nature of the diffusivity changes.

For the creation of the EF composite scores, we carried out a confirmatory factor analysis (CFA) using the robust maximum likelihood estimator. At each time point, test scores from the various EF tests were loaded on to a latent factor. Missing data were handled using full information maximum likelihood. The Root Mean Square Error of Approximation, Comparative Fit Index, Standardized Root Mean square Residual, Akaike Information Criterion, and Bayesian Information Criterion (BIC) were used to assess model fit. Root Mean Square Error of Approximation values of less than 0.05 was considered a good fit. Comparative Fit Index values greater than 0.95 were considered a very good fit (Browne and Cudeck, 1993). Standardized Root Mean square Residual values less than 0.08 are indicative of an acceptable model (Hu and Bentler, 1999). Lower information criterion values correspond to better fit. The longitudinal invariance of the EF factor was tested by comparing the unconstrained and longitudinally invariant (equal unstandardized factor loadings across time) models using the $\chi^2$ test of difference. If the fit was not significantly different between the unconstrained and longitudinally invariant models, the latter model was preferred for it would keep the latent structure of the EF composite score constant throughout both time points. The CFA was carried out using the R package lavaan (Rosseel, 2012). Subsequently, the EF composite scores were extracted from the preferred model's factor scores using the lavPredict function. We proceeded to validate these scores by comparing them between diagnosis groups using a one-way analysis of variance. Post hoc Tukey's tests were subsequently used to determine pairwise differences between groups. We also validated these scores longitudinally by carrying out paired sample t-tests on both groups of participants. Significantly lower baseline EF scores among FTD groups, relative to healthy controls, as well as a significant longitudinal decline in EF scores among bvFTD, but not healthy controls, would suggest the EF composite scores to be criterion valid. These analyses were carried out in R 3.4.0. Statistical significance was set at $p < 0.05$.

## 3. Results

### 3.1. Longitudinal changes in FA and MD

Fig. 1 illustrates the significant clusters of FA and MD changes across time in participants with bvFTD. Table 2 reports the details of these significant clusters. Among participants with bvFTD, significant clusters of FA decrease were observed mainly in the body and genu of the CC, and widespread clusters of MD increase were observed extensively throughout the brain in several WM tracts. There were no

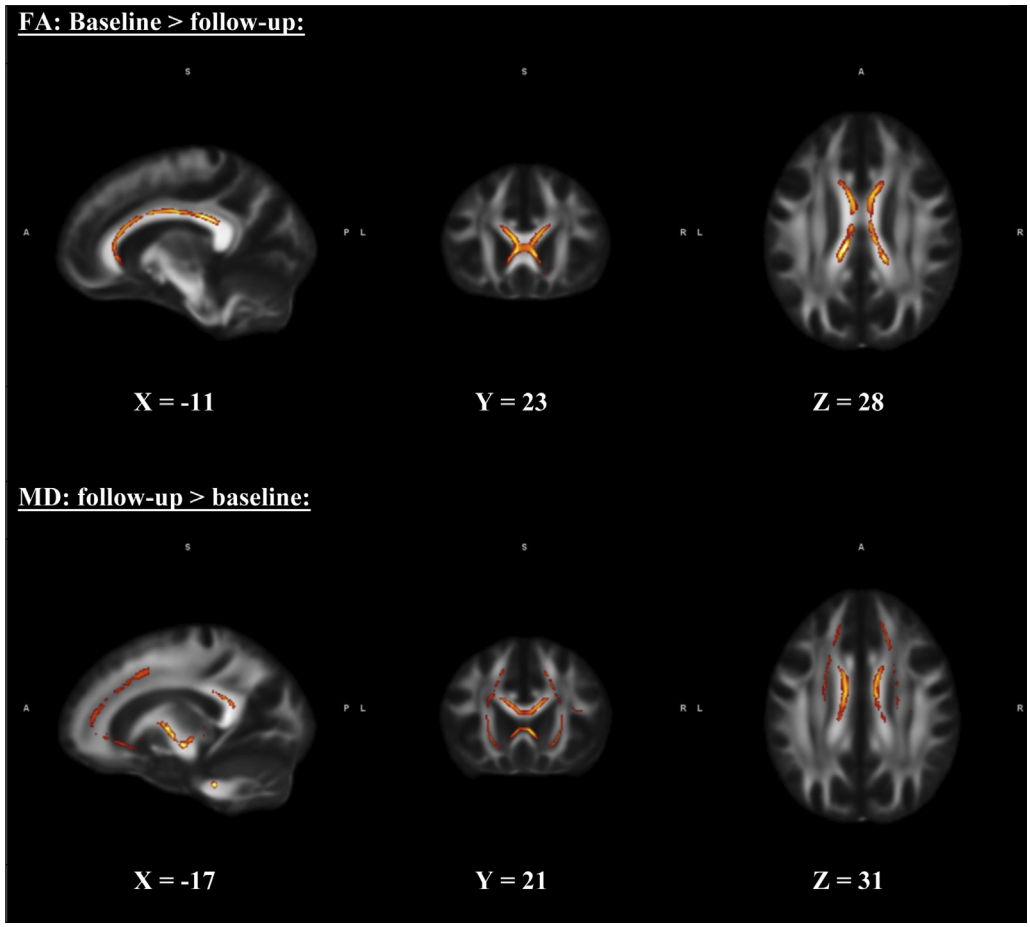


**Fig. 1.** Significant clusters of FA and MD changes in across time in bvFTD patients. Abbreviations: bvFTD, behavioral variant frontotemporal dementia; FA, fractional anisotropy; MD, mean diffusivity.

significant clusters of FA increase or MD decrease among participants with bvFTD. There were also no significant clusters of FA or MD changes in any direction among healthy controls. Next, we attempted to quantify the changes in these significant clusters by first extracting all of the significant clusters as one ROI in their respective contrasts and then compute percentage change (i.e., [follow-up−baseline]/baseline * 100%). From baseline to follow-up, patients with bvFTD experienced a −5.32% (SD = 5.10) and +4.21% (SD = 3.44) change in the FA and MD ROIs, respectively. We also computed the Cohen's d of the absolute change to be 1.07 and 1.17 for FA and MD, respectively. The ROI masks extracted from the bvFTD contrasts were then warped to the study template of the healthy controls before using them to calculate percentage changes in the ROI values in a similar manner. Healthy participants had much smaller changes in the DTI metrics of bvFTD-affected clusters in terms of percentage ($mean_{\Delta FA} = +0.15\%$, SD = 2.36; $mean_{\Delta MD} = +0.26\%$, SD = 1.76) and effect sizes (Cohen's $d_{\Delta FA} = 0.05$; Cohen's $d_{\Delta MD} = 0.14$).

Given the significant MD results, we proceeded to examine RD and AxD changes. Significant clusters of AxD and RD increase were observed extensively throughout the brain in several WM tracts. These results are reported in detail in the supplementary materials (see Fig. S1 and Table S2). The pattern of changes appears to be largely similar between AxD and RD.

### 3.2. Executive function composite score

The fit indices (see Table 3) of the CFA suggested that both the unconstrained and longitudinal invariant models fitted well. Furthermore, the $\chi^2$ test of difference between both models was not significant ($\Delta\chi^2 = 2.83$, $\Delta df = 4$, $p = 0.59$), suggesting that the longitudinal invariance of the EF factor did not significantly worsen the fit of the model. Henceforth, the longitudinal invariant model was used for extracting the EF composite scores. The results of this longitudinal invariant model are presented in Fig. 2. All 3 patient groups had significantly lower EF scores compared to healthy controls ($ps <$ 0.001; see Fig. S2 in the supplementary materials). As expected, among the scanned participants, a significant decline in EF scores was observed among those with bvFTD ($p = 0.006$; Cohen's $d_{\Delta} =$ 0.66) but not healthy controls (see Table 4). These results suggest that the EF composite scores had good external validity.

### 3.3. Longitudinal relationship between EF and DTI metrics

Next, we looked at the longitudinal relationship between WM microstructural changes and EF scores. For this, a single-group average with additional covariates model was used to determine the associations between the FA/MD difference (across time) maps and EF changes, while controlling for age, sex, and education. Fig. 3 illustrates the clusters of FA and MD changes, which were significantly associated with EF changes across time. Table 5 presents information relating to these significant clusters of FA and MD changes. In general, clusters located in the anterior corona radiata (ACR), CC for both FA and MD, were significantly associated with EF changes in their expected directions. Subsequently, this analysis was repeated for RD and AxD; we did not observe any significant RD or AxD clusters in any contrasts. Nevertheless, the uncorrected

**Table 2**
Significant clusters of FA and MD changes across time in participants with bvFTD

| Measure | Contrast | k | *p* | MNI coordinates | | | Labels[a] |
|---|---|---|---|---|---|---|---|
| | | | | X | Y | Z | |
| FA | | | | | | | |
| | Baseline > follow-up | | | | | | |
| | | 94 | 0.004 | −8 | −27 | 26 | Body of corpus callosum |
| | | 89 | 0.003 | 10 | 21 | 20 | Genu of corpus callosum |
| | | 48 | 0.004 | −6 | 21 | 18 | Genu of corpus callosum |
| | | 33 | 0.006 | 7 | 21 | 0 | Genu of corpus callosum |
| | | 31 | 0.003 | 9 | 5 | 29 | Body of corpus callosum |
| | Follow-up > baseline | | | | | | |
| | | No significant clusters | | | | | |
| MD | | | | | | | |
| | Baseline > follow-up | | | | | | |
| | | No significant clusters | | | | | |
| | Follow-up > baseline | | | | | | |
| | | 157 | 0.002 | −32 | −13 | −11 | External capsule R |
| | | 155 | 0.001 | 12 | 22 | 20 | Genu of corpus callosum |
| | | 71 | 0.005 | 30 | −28 | 6 | Retrolenticular part of internal capsule R |
| | | 69 | 0.003 | 32 | 1 | −20 | Uncinate fasciculus R |
| | | 64 | 0.003 | −6 | −28 | 25 | Body of corpus callosum |
| | | 51 | 0.003 | −13 | 22 | 22 | Genu of corpus callosum |
| | | 48 | 0.003 | 23 | 14 | 8 | Anterior limb of internal capsule R |
| | | 48 | 0.004 | 26 | 10 | −9 | External capsule R |
| | | 47 | 0.004 | 16 | 27 | 33 | Body of corpus callosum |
| | | 47 | 0.003 | −21 | 30 | −1 | Anterior corona radiata L |
| | | 43 | 0.004 | 19 | 20 | −6 | External capsule R |
| | | 41 | 0.005 | 9 | −26 | 26 | Body of corpus callosum |
| | | 38 | 0.003 | −14 | 22 | 40 | Anterior corona radiata L |
| | | 38 | 0.004 | −13 | −45 | 16 | Splenium of corpus callosum |
| | | 36 | 0.005 | 17 | −40 | 26 | Splenium of corpus callosum |
| | | 34 | 0.003 | −21 | 23 | 23 | Anterior corona radiata L |
| | | 33 | 0.006 | −27 | −27 | 5 | Retrolenticular part of internal capsule L |
| | | 33 | 0.004 | 7 | 21 | 0 | Genu of corpus callosum |

Key: k, number of voxels; FA, fractional anisotropy; MD, mean diffusivity.
[a] JHU ICBM-DTI-81 White matter labels. Due to the large number of significant clusters, only clusters with k ≥ 30 are reported.

results showed that the direction of associations between RD/AxD and EF changes are consistent with that of MD and EF changes.

We have also carried out a cross-sectional tract-based spatial statistics analysis on the association between EF composite scores and FA/MD. No significant FA or MD clusters were observed in any contrasts. Nevertheless, a marginally significant ($p < 0.08$) MD cluster in the ACR was observed to be negatively associated with EF scores. Further details on these analyses and their results are reported in supplementary materials.

## 4. Discussion

The results of this study provided important longitudinal evidence to support the use of DTI to track the progression of bvFTD and its associated decline in EF. Across a 1-year follow-up period, we observed significantly decreased FA and increased MD in several WM tracts in participants with bvFTD. The fact that no such significant longitudinal changes were observed in a comparable sample of healthy controls suggested that these widespread disruptions in WM microstructural integrity were specific to bvFTD and cannot be attributed to normal aging per se. Most importantly, deterioration in the WM microstructural integrity, especially in the ACR and CC, was significantly associated with the decline in EF.

Our results pertaining to the longitudinal changes in FA and MD among patients with bvFTD are relatively consistent with the findings of previous longitudinal studies (Elahi et al., 2017; Kassubek et al., 2018; Lam et al., 2014; Mahoney et al., 2015) in showing reduced WM microstructural integrity in the CC and the frontal WM across time. Nevertheless, we observed a minor discrepancy between our FA and MD findings; decreased FA was mainly observed in the CC, whereas increased MD was observed in frontal WM tracts such as the uncinate fasciculus and ACR, and other regions as well, in addition to the CC. In relation to this, differences in FA and MD results have been widely reported in other neurocognitive disorders such as amnestic mild cognitive impairment (Yu et al., 2017) and Alzheimer's disease (AD; Sexton et al., 2011). It is plausible that the absolute level of diffusion as measured by MD is a more sensitive marker of WM degeneration relative to FA. FA is a measure of the ratio of anisotropic and isotropic diffusions. Although equivalent increases in both types of diffusion would increase the absolute magnitude of the diffusion ellipsoid as measured by MD, the shape of this ellipsoid or FA would remain a constant (Acosta-Cabronero et al., 2010). Our AxD and RD

**Table 3**
Fit indices of the tested CFA models

| Model | $\chi^2$ (*df*) | CFI | RMSEA | SRMR | AIC | BIC |
|---|---|---|---|---|---|---|
| Unconstrained | 87.70 (27) | 0.960 | 0.080 | 0.051 | 12,964 | 13,108 |
| Longitudinally invariant | 89.42 (31) | 0.962 | 0.074 | 0.059 | 12,959 | 13,088 |

Key: AIC, Akaike Information Criterion; BIC, Bayesian Information Criterion; CFI, Comparative Fit Index; df, degrees of freedom; RMSEA, Root Mean Square Error of Approximation; SRMR, standardized root mean square residual.

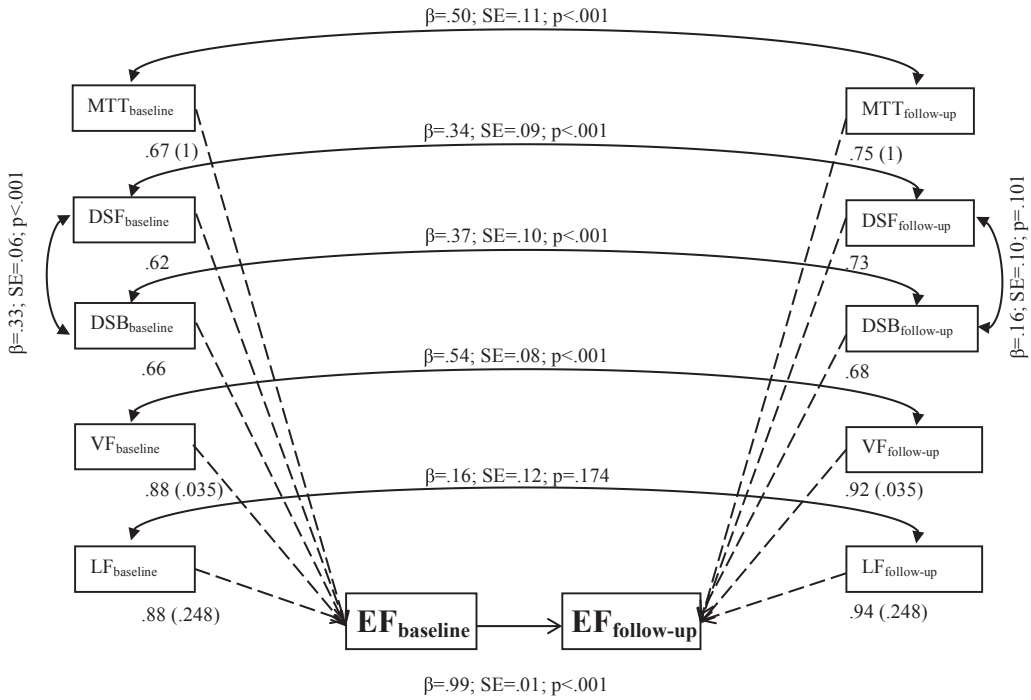


**Fig. 2.** Robust Maximum likelihood estimation of longitudinal confirmatory factor analysis model. The numbers next to dotted lines represent standardized factor loadings (unstandardized factor loadings in parentheses). Straight line represents regression paths. Curve lines represent residual covariance. Abbreviations: DSF, digit span forward; DSB, digit span backward; EF, executive functions; LF, letter fluency; MTT, modified trails test; SE, standard error; VF, verbal fluency; β, standardized coefficients.

results are consistent with such a view. We found that the AxD and RD of several WM tracts were similarly affected in bvFTD, which may provide some evidence to suggest that the shape of the diffusion ellipsoid is relatively less affected and the WM changes in bvFTD are not specific to either radial or axial degeneration.

Although this WM integrity deterioration in bvFTD, as observed via the DTI metrics, may be directly explained by the different types of underlying pathologies described earlier, this degeneration can also be explained by other secondary or indirect disease-related mechanisms. For instance, it is known that patients with bvFTD commonly present with atypical eating habits; this may be associated with increased consumption of high sugar content food (Piguet et al., 2010), which would increase the risk of developing cerebrovascular diseases (Seetharaman, 2016). This will, in turn, result in the appearance of WM hyperintensities in T2-weighted magnetic resonance imaging scans, which will significantly reduce FA and increase MD in affected WM regions (Svärd et al., 2017). Future studies could evaluate such a hypothesis by studying dietary intake and cerebrovascular comorbidities in bvFTD.

Not surprisingly, among patients with bvFTD, the clusters of FA and MD changes correlating with EF decline do share a large overlap, with those of FA and MD changes across time in bvFTD. Interestingly, these WM correlates of EF were not observed in previous cross-sectional studies (Hornberger et al., 2011; Tartaglia et al., 2012). One possible interpretation to emerge from these discrepant findings would be that the other frontal WM tracts such as forceps minor, anterior cingulum, and uncinate fasciculus (at least for FA), which were observed to be significantly correlated with EF in these cross-sectional studies, may represent some other pre-existing vulnerabilities to develop bvFTD or at least EF deficits in general. Hence, these regions do not exhibit significant longitudinal changes in FA and MD nor were they significantly associated with longitudinal EF changes in bvFTD. Of course, other less interesting explanations relating to the methodological differences across studies may explain these inconsistent findings as well. These include the differences in the measurement of EF, acquisition and preprocessing of DTI images, as well as analytical approaches (whole-brain vs. ROI-based). Future longitudinal studies using similar or at least comparable methods on the relationship between EF decline and WM microstructural integrity in bvFTD are required to resolve this uncertainty. Of note, there are several WM tracts (e.g., internal and external capsule) that exhibited a significant decline in integrity across time in bvFTD and were not correlated with EF changes. It remains unclear if these changes are associated with other bvFTD symptoms such as sociocognitive deficits and apathy or simply due to some other pathophysiological processes secondary to the condition. This can only be clarified with future longitudinal research on the relationship between the changes in DTI metrics with other bvFTD symptoms. Finally, the fact that our AxD and RD results in this area did not reveal any significant clusters may be somewhat puzzling considering that significant MD clusters were associated with EF changes. Given the small sample size, it is possible that the study did not have adequate power to detect EF associations with either types of degeneration (axial or radial) but just had enough power to detect EF associations with a combination of both types of degeneration, in the form of MD. Nevertheless, this explanation is at best a speculation, which requires future larger sampled studies to verify.

Our results suggest that the degeneration of CC and ACR to be implicated in the progression of bvFTD, as specifically measured via the decline of EF. The CC is a bundle of WM fibers that connects

**Table 4**
Longitudinal changes in EF scores among scanned participants

| Group | EF scores [M (SD)] | | $t^a$ |
|---|---|---|---|
| | Baseline | Follow-up | |
| Healthy controls | 4.92 (20.19) | 5.92 (24.66) | 1.11 |
| bvFTD | −15.27 (17.56) | −18.14 (21.38) | 3.08[b] |

Key: bvFTD, behavioral variant frontotemporal dementia; EF, executive functions; M, mean; SD, standard deviation.
[a] paired *t*-test.
[b] $p < 0.01$.

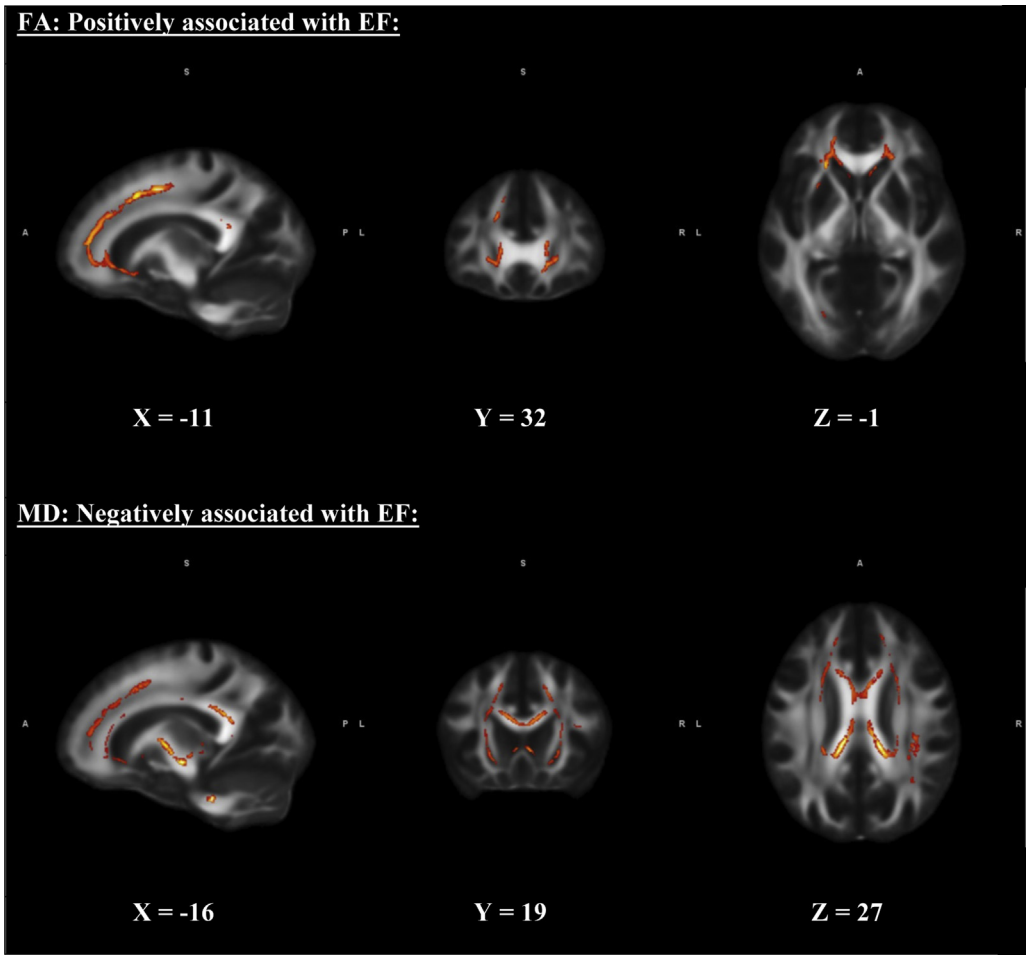


**Fig. 3.** Clusters of FA and MD changes significantly associated with EF changes across time in bvFTD patients. Abbreviations: bvFTD, behavioral variant frontotemporal dementia; FA, fractional anisotropy; MD, mean diffusivity.

between the left and right hemispheres of the brain. Its involvement in bvFTD is not unexpected, given that it subserves several cognitive functions, notwithstanding EF (Kennedy and Raz, 2009; Qiu et al., 2016). In fact, the CC has been implicated in other neurocognitive disorders such as amnestic mild cognitive impairment (Yu et al., 2017) and AD (Sexton et al., 2011). Perhaps the degeneration of the CC may represent more of a general than a specific type of cognitive decline (i.e., that of EF). Speculatively, the degeneration of the ACR may be more specific to bvFTD and or at least EF deficits. The ACR is a bundle of projection fibers within the limbic-thalamo-cortical circuitry. Previous cross-sectional research has associated its microstructural integrity with individual differences in EF among healthy adults (Niogi et al., 2010), adolescents (Seghete et al., 2013), and patients with bipolar disorder (Poletti et al., 2015). Furthermore, results from our further analyses involving DTI metrics and memory composite scores (see supplementary materials) do partially support the idea that the ACR at least for its FA may be more specific to EF deficits. For instance, we observed that memory decline was not significantly associated with any changes in the FA of the ACR, although this decline was significantly associated with the FA in the CC genu. On the other hand, changes in MD was significantly associated with both EF and memory decline for both the CC genu and ACR. These findings also suggest that widespread FA/MD changes are associated with cognitive decline more generally; among these widespread changes, only certain regions of FA/MD changes, such as in the ACR, may be functionally specific.

The implications of these findings are significant. In showing that WM microstructural changes are longitudinally associated with observable cognitive changes in bvFTD, we have essentially validated these WM microstructural changes as a marker of bvFTD progression. In the clinical context, these findings suggest that DTI can be used in conjunction with cognitive assessments to more accurately gauge the progression of bvFTD, so as to predict its prognosis and inform treatment decisions. These findings also pave the way for the future research to more confidently use the DTI modality to investigate the different subgroups of patients with bvFTD, in terms of their different rates of progression. The present study is limited by the relatively short follow-up period and small sample sizes. Nevertheless, it is somewhat remarkable that we found relatively robust effects despite these limitations, which further alludes to the dramatic changes in WM microstructural integrity in bvFTD. Furthermore, we were also unable to examine GM variables in the present study due to limitations with the dataset. As such we did not account for other relevant variables such as frontal lobe atrophy. Future studies should aim to study both GM and WM variables concurrently, so as to obtain a more complete picture on the pattern of neurodegeneration in bvFTD. This would also enable one to determine if either of them is a better predictor of EF decline or that a combination of them would best

**Table 5**
Clusters of FA and MD changes significantly associated with EF changes across time in patients with bvFTD

| Measure | Contrast | k | *p* | MNI coordinates | | | Labels[a] |
|---|---|---|---|---|---|---|---|
| | | | | X | Y | Z | |
| FA | | | | | | | |
| | Positively associated with EF | | | | | | |
| | | 90 | 0.004 | −15 | 37 | 26 | Anterior corona radiata L |
| | | 84 | 0.004 | −20 | 25 | −3 | Anterior corona radiata L |
| | | 36 | 0.014 | −2 | 24 | 8 | Genu of corpus callosum |
| | Negatively associated with EF | | | | | | |
| | | No significant clusters | | | | | |
| MD | | | | | | | |
| | Positively associated with EF | | | | | | |
| | | No significant clusters | | | | | |
| | Negatively associated with EF | | | | | | |
| | | 141 | 0.004 | −22 | 32 | 0 | Anterior corona radiata L |
| | | 112 | 0.008 | −15 | 45 | 16 | Anterior corona radiata L |
| | | 77 | 0.013 | −22 | −40 | 25 | Splenium of corpus callosum |
| | | 77 | 0.006 | −8 | 27 | 12 | Genu of corpus callosum |
| | | 54 | 0.018 | 21 | 28 | −2 | Anterior corona radiata R |
| | | 46 | 0.009 | −22 | 25 | 23 | Anterior corona radiata L |
| | | 41 | 0.015 | −18 | −78 | 8 | Posterior thalamic radiation L |
| | | 39 | 0.015 | −27 | −60 | 11 | Splenium of corpus callosum |

Key: bvFTD, behavioral variant frontotemporal dementia; EF, executive functions; FA, fractional anisotropy; k, number of voxels; MD, mean diffusivity.
[a] JHU ICBM-DTI-81 White matter labels. Due to the large number of significant clusters, only clusters with k ≥ 30 are reported.

predict EF decline. This knowledge will optimize the use of neuroimaging in tracking the progression of bvFTD. Furthermore, if one intends to study bvFTD together with other dementias, the inclusion of GM variables is crucial as one study has shown that the inclusion GM variables would help to differentiate between bvFTD and AD (Möller et al., 2015). Finally, there is some concern that the DTI metrics would be influenced by the partial volume effects associated with GM atrophy. In the present study, these partial volume effects have been largely minimized, given that we have applied a relatively stringent threshold of FA> 0.30 on the mean FA skeleton, and only analyzed voxels, which were projected onto this mean FA skeleton.

### 4.1. Conclusion

Using EF composite scores derived from multiple objective cognitive tests, the present study set out to validate the use of DTI in tracking the progression of bvFTD. Our findings revealed the significant decline across time, in the microstructural integrity of several WM tracts among patients with bvFTD. More importantly, the longitudinal decline in the WM microstructural integrity of the CC and ACR was found to correlate significantly with the decline in EF across time. Taken together, the present study presented valuable longitudinal evidence to support the use of DTI in tracking the progression of bvFTD and its associated EF decline.

## Disclosure

The authors have no actual or potential conflicts of interest.

## Acknowledgements

This work is supported by funding from The University of Hong Kong, Hong Kong May Endowed Professorship and the KKHo International Charitable Foundation. Data collection and sharing for this project was funded by the Frontotemporal Lobar Degeneration Neuroimaging Initiative (National Institutes of Health, United States Grant R01 AG032306). The funders had no involvement in the study design, data collection and analysis, decision to publish, or preparation of the article. The FTLDNI is coordinated through the University of California, San Francisco, Memory and Aging Center. FTLDNI data are disseminated by the Laboratory for Neuro Imaging at the University of Southern California.

## Appendix A. Supplementary data

Supplementary data associated with this article can be found, in the online version, at https://doi.org/10.1016/j.neurobiolaging.2018.12.005.

## References

Acosta-Cabronero, J., Williams, G.B., Pengas, G., Nestor, P.J., 2010. Absolute diffusivities define the landscape of white matter degeneration in Alzheimer's disease. Brain 133, 529–539.
Bang, J., Spina, S., Miller, B.L., 2015. Frontotemporal dementia. Lancet 386, 1672–1682.
Browne, M.W., Cudeck, R., 1993. Alternative ways of assessing model fit. In: Bollen, K.A., Long, J.S. (Eds.), Testing Structural Equation Models. Sage Publications, California, p. 136.
Devenney, E., Bartley, L., Hoon, C., O'Callaghan, C., Kumfor, F., Hornberger, M., Kwok, J.B., Halliday, G.M., Kiernan, M.C., Piguet, O., Hodges, J.R., 2015. Progression in behavioral variant frontotemporal dementia: a longitudinal study. JAMA Neurol. 72, 1501–1509.
Elahi, F.M., Marx, G., Cobigo, Y., Staffaroni, A.M., Kornak, J., Tosun, D., Boxer, A.L., Kramer, J.H., Miller, B.L., Rosen, H.J., 2017. Longitudinal white matter change in frontotemporal dementia subtypes and sporadic late onset Alzheimer's disease. Neuroimage Clin. 16, 595–603.
Ghetti, B., Oblak, A.L., Boeve, B.F., Johnson, K.A., Dickerson, B.C., Goedert, M., 2015. Invited review: frontotemporal dementia caused by microtubule-associated protein tau gene ( MAPT ) mutations: a chameleon for neuropathology and neuroimaging. Neuropathol. Appl. Neurobiol. 41, 24–46.
Gorno-Tempini, M.L., Hillis, A.E., Weintraub, S., Kertesz, A., Mendez, M., Cappa, S.F., Ogar, J.M., Rohrer, J.D., Black, S., Boeve, B.F., Manes, F., Dronkers, N.F., Vandenberghe, R., Rascovsky, K., Patterson, K., Miller, B.L., Knopman, D.S., Hodges, J.R., Mesulam, M.M., Grossman, M., 2011. Classification of primary progressive aphasia and its variants. Neurology 76, 1006–1014.
Hornberger, M., Geng, J., Hodges, J.R., 2011. Convergent grey and white matter evidence of orbitofrontal cortex changes related to disinhibition in behavioural variant frontotemporal dementia. Brain 134, 2502–2512.
Hu, L., Bentler, P.M., 1999. Cutoff criteria for fit indexes in covariance structure analysis: Conventional criteria versus new alternatives. Struct Equ Model A Multidiscip J 6, 1–55.
Irwin, D.J., McMillan, C.T., Brettschneider, J., Libon, D.J., Powers, J., Rascovsky, K., Toledo, J.B., Boller, A., Bekisz, J., Chandrasekaran, K., Wood, E.M., Shaw, L.M., Woo, J.H., Cook, P.A., Wolk, D.A., Arnold, S.E., Van Deerlin, V.M., McCluskey, L.F., Elman, L., Lee, V.M.Y., Trojanowski, J.Q., Grossman, M., 2012. Cognitive decline and reduced survival in C9orf72 expansion frontotemporal degeneration and amyotrophic lateral sclerosis. J. Neurol. Neurosurg. Psychiatry 84, 163–169.

Kassubek, J., Müller, H.P., Tredici, K. Del, Hornberger, M., Schroeter, M.L., Müller, K., Anderl-Straub, S., Uttner, I., Grossman, M., Braak, H., Hodges, J.R., Piguet, O., Otto, M., Ludolph, A.C., 2018. Longitudinal diffusion tensor imaging resembles patterns of pathology progression in behavioral variant frontotemporal dementia (bvFTD). Front. Aging Neurosci. 10, 47.

Keihaninejad, S., Zhang, H., Ryan, N.S., Malone, I.B., Modat, M., Cardoso, M.J., Cash, D.M., Fox, N.C., Ourselin, S., 2013. An unbiased longitudinal analysis framework for tracking white matter changes using diffusion tensor imaging with application to Alzheimer's disease. Neuroimage 72, 153–163.

Kennedy, K.M., Raz, N., 2009. Aging white matter and cognition: differential effects of regional variations in diffusion properties on memory, executive functions, and speed. Neuropsychologia 47, 916–927.

Kramer, J.H., Jurik, J., Sha, S.J., Rankin, K.P., Rosen, H.J., Johnson, J.K., Miller, B.L., 2003. Distinctive neuropsychological patterns in frontotemporal dementia, semantic dementia, and Alzheimer disease. Cogn. Behav. Neurol. 16, 211–218.

Lam, B.Y.K., Halliday, G.M., Irish, M., Hodges, J.R., Piguet, O., 2014. Longitudinal white matter changes in frontotemporal dementia subtypes. Hum. Brain Mapp. 35, 3547–3557.

Leyns, C.E.G., Holtzman, D.M., 2017. Glial contributions to neurodegeneration in tauopathies. Mol. Neurodegener. 12, 50.

Lezak, M.D., 1995. Neuropsychological Assessment, third ed. Oxford University Press, New York .

Mackenzie, I.R.A., Neumann, M., 2016. Molecular neuropathology of frontotemporal dementia: insights into disease mechanisms from postmortem studies. J. Neurochem. 138, 54–70.

Mahoney, C.J., Simpson, I.J.A., Nicholas, J.M., Fletcher, P.D., Downey, L.E., Golden, H.L., Clark, C.N., Schmitz, N., Rohrer, J.D., Schott, J.M., Zhang, H., Ourselin, S., Warren, J.D., Fox, N.C., 2015. Longitudinal diffusion tensor imaging in frontotemporal dementia. Ann. Neurol. 77, 33–46.

Mann, D.M.A., Snowden, J.S., 2017. Frontotemporal lobar degeneration: pathogenesis, pathology and pathways to phenotype. Brain Pathol. 27, 723–736.

Möller, C., Hafkemeijer, A., Pijnenburg, Y.A.L., Rombouts, S.A.R.B., Van Der Grond, J., Dopper, E., Van Swieten, J., Versteeg, A., Pouwels, P.J.W., Barkhof, F., Scheltens, P., Vrenken, H., Van Der Flier, W.M., 2015. Joint assessment of white matter integrity, cortical and subcortical atrophy to distinguish AD from behavioral variant FTD: a two-center study. Neuroimage Clin. 9, 418–429.

Neary, D., Snowden, J.S., Gustafson, L., Passant, U., Stuss, D., Black, S., Freedman, M., Kertesz, A., Robert, P.H., Albert, M., Boone, K., Miller, B.L., Cummings, J., Benson, D.F., 1998. Frontotemporal lobar degeneration: a consensus on clinical diagnostic criteria. Neurology 51, 1546–1554.

Niogi, S., Mukherjee, P., Ghajar, J., McCandliss, B.D., 2010. Individual differences in distinct components of attention are linked to anatomical variations in distinct white matter tracts. Front. Neuroanat. 4, 2.

Piguet, O., Petersén, Å., Yin Ka Lam, B., Gabery, S., Murphy, K., Hodges, J.R., Halliday, G.M., 2010. Eating and hypothalamus changes in behavioral-variant frontotemporal dementia. Ann. Neurol. 69, 312–319.

Piguet, O., Hornberger, M., Mioshi, E., Hodges, J.R., 2011. Behavioural-variant frontotemporal dementia: diagnosis, clinical staging, and management. Lancet Neurol. 10, 162–172.

Poletti, S., Bollettini, I., Mazza, E., Locatelli, C., Radaelli, D., Vai, B., Smeraldi, E., Colombo, C., Benedetti, F., 2015. Cognitive performances associate with measures of white matter integrity in bipolar disorder. J. Affect. Disord. 174, 342–352.

Powers, J.M., Byrne, N.P., Ito, M., Takao, M., Yankopoulou, D., Spillantini, M.G., Ghetti, B., 2003. A novel leukoencephalopathy associated with tau deposits primarily in white matter glia. Acta Neuropathol. 106, 181–187.

Qiu, Y., Liu, S., Hilal, S., Loke, Y.M., Ikram, M.K., Xu, X., Yeow Tan, B., Venketasubramanian, N., Chen, C.L.H., Zhou, J., 2016. Inter-hemispheric functional dysconnectivity mediates the association of corpus callosum degeneration with memory impairment in AD and amnestic MCI. Sci. Rep. 6, 1–12.

Rascovsky, K., Hodges, J.R., Knopman, D., Mendez, M.F., Kramer, J.H., Neuhaus, J., Van Swieten, J.C., Seelaar, H., Dopper, E.G.P., Onyike, C.U., Hillis, A.E., Josephs, K.A., Boeve, B.F., Kertesz, A., Seeley, W.W., Rankin, K.P., Johnson, J.K., Gorno-Tempini, M.L., Rosen, H., Prioleau-Latham, C.E., Lee, A., Kipps, C.M., Lillo, P., Piguet, O., Rohrer, J.D., Rossor, M.N., Warren, J.D., Fox, N.C., Galasko, D., Salmon, D.P., Black, S.E., Mesulam, M., Weintraub, S., Dickerson, B.C., Diehl-Schmid, J., Pasquier, F., Deramecourt, V., Lebert, F., Pijnenburg, Y., Chow, T.W., Manes, F., Grafman, J., Cappa, S.F., Freedman, M., Grossman, M., Miller, B.L., 2011. Sensitivity of revised diagnostic criteria for the behavioural variant of frontotemporal dementia. Brain 134, 2456–2477.

Rosseel, Y., 2012. lavaan: An R Package for Structural Equation Moeling. J. Stat. Software 1 (2). https://doi.org/10.18637/jss.v048.i02.

Seetharaman, S., 2016. Chapter 24 - The influences of dietary sugar and related metabolic disorders on cognitive aging and dementia. In: Malavolta, M. (Ed.), Molecular Basis of Nutrition and Aging. Academic Press, San Diego, pp. 331–344.

Seghete, K.L.M., Herting, M.M., Nagel, B.J., 2013. White matter microstructure correlates of inhibition and task-switching in adolescents. Brain Res. 1527, 15–28.

Sexton, C.E., Kalu, U.G., Filippini, N., Mackay, C.E., Ebmeier, K.P., 2011. A meta-analysis of diffusion tensor imaging in mild cognitive impairment and Alzheimer's disease. Neurobiol. Aging 32, 2322.e5–2322.e18.

Svärd, D., Nilsson, M., Lampinen, B., Lätt, J., Sundgren, P.C., Stomrud, E., Minthon, L., Hansson, O., van Westen, D., 2017. The effect of white matter hyperintensities on statistical analysis of diffusion tensor imaging in cognitively healthy elderly and prodromal Alzheimer's disease. PLoS One 12, e0185239.

Tartaglia, M.C., Zhang, Y., Racine, C., Laluz, V., Neuhaus, J., Chao, L., Kramer, J., Rosen, H., Miller, B., Weiner, M., 2012. Executive dysfunction in frontotemporal dementia is related to abnormalities in frontal white matter tracts. J. Neurol. 259, 1071–1080.

Wechsler, D., 1997. Wechsler Adult Intelligence Scale. Psychological Corporation, San Antonio, TX.

Winkler, A.M., Ridgway, G.R., Webster, M.A., Smith, S.M., Nichols, T.E., 2014. Permutation inference for the general linear model. Neuroimage 92, 381–397.

Yu, J., Lam, C.L.M., Lee, T.M.C., 2017. White matter microstructural abnormalities in amnestic mild cognitive impairment: a meta-analysis of whole-brain and ROI-based studies. Neurosci. Biobehav. Rev. 83, 405–416.

Zhang, Y., Tartaglia, M.C., Schuff, N., Chiang, G.C., Ching, C., Rosen, H.J., Gorno-Tempini, M.L., Miller, B.L., Weiner, M.W., 2013. MRI signatures of brain macrostructural atrophy and microstructural degradation in frontotemporal lobar degeneration subtypes. J. Alzheimers Dis. 33, 431–444.